symmetry

Article

Beam Asymmetry, Divergence and Energy Spread Effects on the Radiation from Planar Undulators

Konstantin Zhukovsky * and Igor Fedorov

Department of Theoretical Physics, Faculty of Physics, M.V. Lomonosov Moscow State University, 119991 Moscow, Russia; fedorov.ia15@physics.msu.ru

* Correspondence: zhukovsk@physics.msu.ru; Tel.: +7-(495)9393177

Abstract: The theoretical study of the effect of electron beam parameters, in particular, the emittance and its asymmetry on the radiation from relativistic electrons in undulators is conducted both analytically and numerically. The reasons for the odd and even harmonic generation and radiation are explored. The difference in the underlying physical reasons for the spontaneous and stimulated radiation of harmonics in free electron lasers (FELs) is elucidated. The generalized forms of the special functions of the Bessel and Airy type are employed to account analytically for the off-axis and angular effects together with the effect of the beam energy spread. A comparative analysis of the radiation spectra for undulators with different beams is performed. The examples of the radiation at SPARC and LEUTL are given. The effect of the asymmetry of the beam on the radiation properties is analyzed. The alternative theoretical approaches of other authors are also employed for the analytical calculation of the harmonic powers in FELs. The results are compared with existing experimental data.

Keywords: radiation; harmonics; undulator; free electron laser; electron beam

check for updates

Citation: Zhukovsky, K.; Fedorov, I. Beam Asymmetry, Divergence and Energy Spread Effects on the Radiation from Planar Undulators. *Symmetry* **2022**, *14*, 1353. https://doi.org/10.3390/sym14071353

Academic Editor: Anna Cimmino

Received: 5 May 2022
Accepted: 23 June 2022
Published: 30 June 2022

Publisher's Note: MDPI stays neutral with regard to jurisdictional claims in published maps and institutional affiliations.

Copyright: © 2022 by the authors. Licensee MDPI, Basel, Switzerland. This article is an open access article distributed under the terms and conditions of the Creative Commons Attribution (CC BY) license (https://creativecommons.org/licenses/by/4.0/).

1. Introduction

The radiation from relativistic electrons in a spatially periodic magnetic field was first obtained and explored by Motz [1], following the hypothesis of Ginzburg [2]. It was named undulator radiation (UR) as it was generated in a device, called an undulator; the UR is incoherent. The coherent radiation from electrons in undulators was discovered by Madey [3] few decades after the discovery of the UR. Madey also developed a theory, that described the interaction of electrons with the radiation in the undulator and consequent grouping of the electrons in microbunches, whose lengths are shorter than the wavelength of the radiation. This was the theory for the coherent radiation in free electron lasers (FELs), whose main elements are the undulator and a high quality beam of quasi-monoenergetic electrons. In the 21st century, FEL radiation is used for studies in various branches of science. The theory and applications are well described in literature (see, for example, [4–10] etc.). FELs are the fourth generation of radiation sources and they represent ulterior development of the third generation sources—electron storage rings [11–14]. The principle of a FEL is based on the phenomenon that electrons in an undulator lag slightly behind the wave of the radiation and the appearing lag is such that the Lorenz force always pushes electrons toward the nodes of the UR wave in the undulator. Thus bunching occurs at the radiation wavelength; similarly, bunching occurs also at the harmonic wavelengths, but it is weaker and more sensitive to all kind of losses related to the diffraction, imperfections of the assembly and alignment, magnetization errors, beam energy spread, divergence etc. In the high frequency range, such as UV- and X-rays, particularly tight requirements for beams must be fulfilled for the FEL to operate properly. Moreover, in the X-ray band few materials are capable of reflecting efficiently and the most common construction of a UV- and X-ray

FEL is a single pass design, where the radiation interacts with electrons during one pass along the FEL. The wavelengths of the UR resonances read as follows:

$$\lambda_n = \frac{\lambda_u}{2n\gamma^2}\left(1 + \frac{k_{eff}^2}{2} + (\gamma\Theta)^2\right), \quad (1)$$

where n is the harmonic number, Θ is the off-axis angle, $k_{eff}^2 = k^2\varpi$ is the undulator parameter, $k = H_0\lambda_u e/2\pi mc^2 \approx 0.9337 H_0[\mathrm{T}]\lambda_u[\mathrm{cm}]$, $\varpi = 1 + (d/h)^2$, H_0 is the magnetic field amplitude on the undulator axis, whose typical value is H_0~1 T, dH_0 is the field harmonic amplitude if present in the undulator, whose typical value is small, d << 1, and h is the field harmonic number, e is the electron charge, and λ_u is the undulator period, whose typical value is λ_u~1–3 cm. For the UR in visible range the electron energy has a typical value of ~0.1–0.2 GeV, a γ–factor of ~10^2, and a total undulator length of a dozen meters, for the X-ray FEL, the undulator lengths reaches 100 m and the beam energy E~5–15 GeV, γ~10^4. Modern installations use beams with low energy spread of σ_e~10^{-3}–10^{-4}; the emittances vary: $\varepsilon_{x,y}$~0.5–25 mm $\times$ mrad and beam sections are typically $\sigma_{x,y}$~10–300 μm. The on-axis spectrum of the UR is determined mainly by the undulator; for a planar undulator with an ideal beam it consists of odd harmonics and even harmonics appear off the axis. In real undulators even harmonics are also radiated on the axis. This is due to several reasons, mainly the finite emittance of the beam and the betatron oscillations in the beam. For FEL radiation, the harmonic content is usually smaller than that for the spontaneous UR from the same undulator; in a single pass FEL usually the second, third and sometimes fifths harmonics are radiated. This is due to the nature of FEL radiation, driven by the electron-photon interaction, which is more sensitive to losses at higher harmonic wavelengths. In addition, FEL radiation requires good beams with the conditions for the emittance $\varepsilon_{x,y} \leq \lambda_0/4\pi$ and for the energy spread $\sigma_e \leq \rho/2$ (see [4–10]); in practice they are not always satisfied, but in weaker conditions, $\varepsilon_{x,y}$~$\lambda_0/4\pi$ and $\sigma_e \approx \rho_n$, the generation may be possible. Typically, the single pass FEL radiation spectrum has the third harmonic content ○1–2%, second harmonic: ○0.1%, (see, for example, [15–19]), and the fifth harmonic is rarely detected. Computation of a FEL harmonic power evolution is a complex engineering problem, which is solved by numerical simulations in special programs [20–22]. It requires prepared technical personnel and good computational facilities. Numerical solutions to a set of equations for the motion of the charges, their interaction and energy exchange with the wave, usually yield FEL powers with an accuracy of one order of magnitude for the fundamental and one–two orders of magnitude for the harmonics as compared with the measurements. This is a quite good result, considering that technical procedures, such as adjustment of the magnet pole strengths along the undulators, alignment of the beam and other fine tuning procedures can change the harmonic powers by approximately the same value. Moreover, in a numerical simulation it is difficult to trace the exact effect of each parameter of the beam and undulator on the final harmonic power and such analysis requires highly experienced personnel. A simple alternative way to estimate and analyze FEL harmonic behavior employs the analytical modeling of FEL harmonics evolution. Exact analytical solutions are not available for FELs because of the large number of particles and equations, but our phenomenological modelling gives results with close to numerical simulation accuracy. It is based on some early studies in [23–26] and in its current form it involves all main parameters, and accounts for main losses and variable sensitivity of the electron-photon interaction, dependently on harmonic numbers. It was calibrated with all available data for major FELs in the range from visible to hard X-rays and agrees with the data for operating FELs and with results of numerical simulations [20,21,27–29]. The analytical approach allows the tracing of the effects of each parameter on the harmonic radiation and thus it reveals the underlying physical reasons for the harmonics.

In what follows we will analyze the harmonic radiation in the undulators of several free electron lasers: SPARC [19], "Sorgente Pulsata ed Amplificata di Radiazione Coerente", i.e., Pulsed and Amplified Source of Coherent Radiation, LEUTL [17,18], "Low-Energy

Undulator Test Line", and LCLS [15,16], "Linac Coherent Light Source", and compare the results for the spontaneous and stimulated UR with existing data for FELs and numerical simulations for the spontaneous UR. We will explain the reasons for the proper harmonic content and spectrum with the beam and undulator data.

2. Analytical Estimates for the Harmonic Powers Using Bessel Coefficients

The analytical tool for the study of the UR is based on the formalism of the generalized Bessel functions. In the most general case it involves very complex integrals to account for field harmonics and the resulting expressions can be rather cumbersome when multiple field harmonics in both directions are considered for the radiation off the undulator axis (see for details, for example, [28–39]). In most cases, however, single period planar undulators are used with weak field harmonic content; it has minor effect on the radiation. In this common case the account for the angular and other effects is much simpler. The intensity of UR from one electron is given by the following well-known formula, which goes back to the well-known radiation formulae, for example, in [30]:

$$\frac{d^2 I}{d\omega d\Omega} \cong \frac{e^2\gamma^2 N^2 k^2}{c\left(1+\left(k_{eff}^2/2\right)+(\gamma\theta)^2\right)} \sum_{n=-\infty}^{\infty} n^2 \mathrm{sinc}^2\left(\frac{\nu_n}{2}\right)\left(f_{n;x}^2+f_{n;y}^2\right), \tag{2}$$

where $\nu_n = 2\pi n N((\omega/\omega_n) - 1)$ is the detuning parameter from the resonance $\omega_n = 2\pi c/\lambda_n$; the Bessel coefficients $f_{n;x,y}$ for the x- and y-polarizations depend on the parameters of the beam and the undulator. Omitting the field harmonics effect, which is a stand-alone subject addressed in [23,25,26,31], et al., the Bessel coefficients $f_{n;x,y}$ in (2) reduce for a planar undulator to the following rather simple form:

$$\begin{aligned} f_{n;x} &= \sum_p \widetilde{J}_p \left| \left(J_{n+1}^n + J_{n-1}^n\right) + \tfrac{2}{k}\gamma\theta\cos\varphi J_n^n \right|, \\ f_{n;y} &= \sum_p \left(\widetilde{J}_p \left|\tfrac{2}{k}\gamma\theta\sin\varphi J_n^n\right| + J_n^n \tfrac{\sqrt{2}\pi y_0}{\lambda_u}\left(\widetilde{J}_{p+1} - \widetilde{J}_{p-1}\right)\right), \end{aligned} \tag{3}$$

where we explicitly account for the finite beam size y_0 and for the effects of the off-axis angle θ. The summation over p accounts for all betatron harmonics with numbers p; φ is the polar angle around the undulator axis and J_n^m and $\widetilde{J}_p$ are the Bessel functions, which implicitly account for the angular effects and the beam size in their arguments as follows:

$$\begin{aligned} & J_n^m \equiv J_n^m(\zeta,\xi) \cong \int_{-\pi}^{\pi} \tfrac{d\alpha}{2\pi} \exp[i(n\alpha + m\zeta\sin\alpha + m\xi\sin(2\alpha))], \\ & \zeta = \theta\cos\varphi \tfrac{\lambda_u k}{n\lambda_n\gamma}, \xi = \tfrac{\lambda_u k^2}{8n\lambda_n\gamma^2}, \end{aligned} \tag{4}$$

$$\widetilde{J}_p \equiv J_p^1(-\tau,-\varsigma), \tau = \frac{4\pi\theta y_0\gamma^2}{\lambda_u(1+(k^2/2))}, \varsigma = \frac{\pi^2\gamma y_0^2 k}{\sqrt{2}\lambda_u^2(1+(k^2/2))}. \tag{5}$$

Generalized forms of the special functions that we use contain integrals of elementary functions and in some cases they can be taken by the program Mathematica analytically for the given initial parameters. However, in most cases the integral is evidently best taken by standard numerical procedures in the same Mathematica or another program. We use numerical calculations of the same Mathematica and get results instantly. Note that the calculation of the integral of these integrals, such as, for example, (6), may take a second, and numerical calculation of more cumbersome integral (8) may take a minute or so; times vary, dependently on the hardware.

Betatron oscillations in a finite-sized real beam split each radiation line of the harmonic n at the frequency $\omega_n = 2\pi c/\lambda_n$ into an array of betatron radiation harmonics, which are distant from each other by $\omega_\beta \cong \frac{\omega_n k}{\sqrt{2}n\gamma}$ (see, for example, [40]). Since $\omega_\beta \propto \omega_n/\gamma$, it is evident that $\omega_\beta << \omega_n$ for relativistic electrons with γ >>1, and thus the split of each radiation line occurs in very fine betatron lines close to each other within the line of the harmonic n. The degree of the split depends on the beam and to some extend also on the undulator parameters. Expressions (3) for the Bessel coefficients and integrals (4) for the Bessel functions are used for both the spontaneous and the stimulated radiation analysis. Note, that the angular dependence in (3)–(5) is explicit for the Bessel coefficients, but the broadening effect of the UR lines is not yet described by it; neither is the broadening caused by the energy spread accounted for in (2).

Simple and accurate account for the effect of the finite energy spread σ_e in electron beams can be done by the following common convolution, taken along the undulator with N periods:

$$\frac{d^2 I(\sigma_e)}{d\omega d\Omega} = \int_{-\infty}^{+\infty} d^2 I(\nu_n + 4\pi n N\varepsilon) e^{-\varepsilon^2/2\sigma_e^2} d\varepsilon / d\omega d\Omega \sqrt{2\pi}\sigma_e, \tag{6}$$

the non-periodic dipole magnetic component $H_d = \kappa_1 H_0$, where H_0 is the amplitude of the field $H_0 \sin k_\lambda z$ on the undulator z-axis, $\kappa_1 = \sqrt{\kappa^2 + \rho^2}$, $\rho = H_{d,x}/H_0$, $\kappa = H_{d,y}/H_0$, may appear due to imperfections, magnetizing errors, external fields etc. It causes synchrotron-like effect: bends the electrons trajectory into the effective angle $\theta_H = \frac{2\pi}{\sqrt{3}} \frac{k}{\gamma} N\kappa_1$ [41–44]; its effect is accumulated along the undulator length. Off the undulator axis in the angle θ, the interplay with θ_H appears. The UR line broadens and the red-shift of the resonances appear (see [43,44]). The resonances are as follows:

$$\omega_{\mathrm{n}} = \frac{2n\omega_0\gamma^2}{1 + \frac{k_{eff}^2}{2} + (\gamma\theta)^2 + (\gamma\theta_H)^2 - \gamma^2\theta_H\theta\sqrt{3}\frac{\rho\sin\phi - \kappa\cos\phi}{\kappa_1}}, \tag{7}$$

where φ is the polar angle. The shape of the UR line is described by the generalized Airy-type function $S(\nu_n, \eta, \beta) \equiv \int_0^1 e^{i(\nu_n\tau + \eta\tau^2 + \beta\tau^3)} d\tau$ (see [41–45]). Differently from the effect of the energy spread and associated with it symmetric broadening, the angular effects cause asymmetrical broadening and red shift. The stronger the H_{d}, the more the degradation of the spectral line shape. The last term in the denominator of (7) describes the interplay of the off-axis angle θ and the induced angle θ_H. It follows from (7) that θ_H can in part compensate the spectrum for the deviation of the beam in angle θ: maximum compensation reches $\theta/2$, if the field H_{d} induces the angle $\widetilde{\theta}_H = \mp\theta\frac{\sqrt{3}}{2}\frac{\kappa}{\kappa_1}$ for φ = 0,π, and $\widetilde{\theta}_H = \pm\theta\frac{\sqrt{3}}{2}\frac{\rho}{\kappa_1}$ for $\varphi = \pm\pi/2$.

We omit cumbersome convolution for the UR intensity, which involves the integral form of the generalized Airy-type function for conciseness and also because engineers usually screen out or compensate for non-periodic fields after calculating field integrals. However, the angular effects that are due to the emittance or misalignment of the beam remain and they can also be perceived on the axis. Omitting the dipole fields, only the term $\sim\tau$ remains in the exponential of the Airy-type functions [41–44] and complex convolution for the differential UR intensity simplifies to the following formula, where only the angular effects and the energy spread are accounted for:

$$\begin{aligned}\frac{d^2 I(\theta,\sigma_e)}{d\omega d\Omega} &\cong \frac{e^2\gamma^2 N^2 k^2}{c\left(1+\left(k_{eff}^2/2\right)+\gamma^2\theta^2\right)} \times \\ &\sum_{n=-\infty}^{\infty} n^2\left(f_{n;x}^2 + f_{n;y}^2\right) \int_{-\infty}^{\infty} \frac{d\varepsilon e^{-\varepsilon^2/2\sigma_e^2}}{\sqrt{2\pi}\sigma_e} \left(\int_0^1 \exp\left\{ i\tau\left(\begin{array}{c}\nu_n + 4\pi n N\varepsilon + \\ \frac{2\pi n N(\gamma\theta)^2}{1+\left(k_{eff}{}^2/2\right)+(\gamma\theta)^2}\end{array}\right)\right\} d\tau\right)^2.\end{aligned} \tag{8}$$

For a real beam further integration over the angles should be performed with proper distribution across the beam, such as, for example, Gaussian. However, the effective values for the divergences can be used instead for a simpler estimate. This appears in good agreement with numerical results. Moreover, the difference in the UR intensity computed with (8) and (6) is usually minor, so that common simple expression (6) is good in most cases. However, it is not always so. In what follows we will demonstrate that for the UR from some electron beams with large emittance, the difference between the harmonic intensities obtained with (6) and (8) can be non indifferent and the results from (8) appear much closer to the numerical results, where all effects are carefully included in the numerical modelling. Equation (8) analytically describes the harmonic content and the individual spectrum line broadening for the radiation from the undulator of N periods, affected by the energy spread and angular effects of the beam with finite section. The harmonic radiation is more sensitive to all kind of losses than the radiation at the fundamental. This sensitivity is even higher for the harmonics of free electron lasers, where the electron-photon interaction at the harmonic lengths matters. In what follows it is addressed phenomenologically in the framework of the analytical model for FEL radiation, where the same Bessel coefficients $f_{n;x,y}$ as above are used.

Omitting the detailed description of the phenomenological model for FEL harmonics, based on the early versions in [46,47] and presented in its current form in recent publications (see [23–26,28–39]), we briefly outline that in a FEL the interaction of the radiation with electrons in the undulator causes qualitative change of the power growth along undulators. The quadratic growth at the beginning of a FEL, where the spontaneous radiation dominates, changes to the exponential growth $P(z) \propto P_0 e^{z/L_{g0}}$ of the power from bunched electrons; the initial power is P_0, and it can originate from a seeding laser in an amplifier FEL or from coherent fluctuations of the initial noise of a bunch in a SASE FEL; in the latter case it reads as follows: $P_{n,noise} \approx 1.6\rho_n^2 e 4\pi c P_{beam}/(I_0\lambda_n)$ [48]. The FEL gain length $L_{g0} = 1/\sqrt{3}g_0$ is reciprocal to the gain g_0 and related to the Pierce parameter $\rho = (\lambda_u g_0)/4\pi$ [4–7]. The latter is defined by the properties of the undulator, k_{eff}, λ_u, the Bessel coefficients $f_{n;x,y}$ for the n-th harmonic, and by the relativistic factor γ of the beam, its current I_0 and the beam its cross section Σ (see [4–10]):

$$\rho_n = \frac{1}{2\gamma}\left(\frac{I_0/\Sigma}{4\pi i}\right)^{1/3}\left(\lambda_u k_{eff}|f_n|\right)^{2/3}, \tag{9}$$

where $i = 4\pi\varepsilon_0 mc^3/e \cong 1.7045 \times 10^4$ is the Alfven current dimensional constant [A] and Σ is related to beam emittances $\varepsilon_{x,y}$, Twiss parameters $\beta_{x,y}$, divergences $\theta_{x,y}$ and beam sections $\sigma_{x,y}$ as follows:

$$\Sigma = 2\pi\sigma_x\sigma_y,\ \sigma_{x,y} = \sqrt{\varepsilon_{x,y}\beta_{x,y}},\ \sigma_{x,y} = \varepsilon_{x,y}/\theta_{x,y},\ \theta_{x,y} = \sqrt{\varepsilon_{x,y}/\beta_{x,y}} \tag{10}$$

Losses arise from diffraction, energy spread, emittance etc.; they have detrimental effect on the FEL radiation. While the effect on the spontaneous UR can be quantified precisely in a convolution (8) or in more complex formulae, the exact analytical account for FELs can not be done because of the complexity of the problem, involving equations for the electrons, radiation and their interaction in the undulator. Phenomenological approximations were developed for it. Excellent accurate analytical formula of Ming Xie [49,50] gives correction to the gain length: $L_g = L_{g0}(1+\Lambda)$, where Λ is the polynomial with 19 coefficients for the factors and fractional powers of the terms. This correction is in very good agreement with measurements, but it is cumbersome and proper expressions for the harmonics become even more cumbersome. Good agreement with the approximation of Ming Xie can be achieved by using the accordingly corrected Pierce parameter $\widetilde{\rho} = \rho/\kappa$ [46,47]:

$$\rho_n \to \widetilde{\rho}_n = \rho_n/\kappa, \kappa = \sqrt[3]{1 + \frac{\lambda_u\lambda_n}{16\pi\rho_n\Sigma}}. \tag{11}$$

With modified Pierce parameter ρ_n the theoretical gain length $L^0_{n,g} \cong \lambda_u/\left(4\pi\sqrt{3}n^{1/3}\rho_n\right)$ increases and agrees with that of Xie; the saturated length also increases and the maximum theoretical harmonic power in the regime of the independent harmonic growth, $P_{F,n} \approx \sqrt{2}\rho_n P_{beam}$, where $P_{beam} = EI_0$ is the beam power, decreases. Expressions for the gain, saturation and power read respectively as follows [46,47]:

$$L_{n,g} = L^0_{n,g}\kappa\Phi_n,\ L_s \cong 1.07 L_g \ln\frac{9\eta_1 P_F}{P_0},\ P_{n,F} \cong \sqrt{2}\frac{\eta_1}{\kappa^2}\rho_n P_{beam}, \tag{12}$$

where the effects of the energy spread σ_ε and the emittance $\varepsilon_{x,y}$ are phenomenologically described by the coefficients, and verified for FELs in the wide radiation range from infrared to hard X-rays [25–37]:

$$\begin{array}{l} \Phi_n \cong \left(\zeta^{\sqrt{n}} + 0.165\mu^2_{\varepsilon,n}\right)e^{0.034\mu^2_{\varepsilon,n}},\ \mu_{\varepsilon,n} \cong \frac{2\sigma_\varepsilon}{n^{1/3}\tilde{\rho}_n}, \\ \eta_n \cong 0.942\left(e^{-\Phi_n(\Phi_n-0.9)} + \frac{1.57(\Phi_n-0.9)}{\Phi_n^3}\right). \end{array} \tag{13}$$

The coefficient ζ describes the effect of the emittance and it is usually close to unity, $\zeta \cong 1 - 1.03$, for a matched beam; rarely for beams with large emittances can it increase to $\zeta \approx 1.1 - 1.2$; general expression is very cumbersome, it can be found in [47] and we omit it for brevity. The effect of ζ on the second and third harmonics is usually minor, while for the fundamental it is negligible. However, for large emittances, a proper account should be done with ζ just as we use convolution (8) instead of (6) in this case for the spontaneous UR intensity. The details of the phenomenological model can be found in our preceding publications (see, for example, [32–39]).

The harmonic power in the nonlinear generation is induced by the fundamental; the respective harmonic power grows faster, $\propto e^{nz/L_g}$, than its independent growth $\propto e^{z/L_{n,g}}$ [4–10,47,48,51]. The saturation of a FEL occurs usually because of the fundamental, because $L_{n,g} > L_{1,g}$ and the saturated harmonic powers in the nonlinear generation are lower than the saturated powers harmonic in the independent growth; the latter can be reached farther along the undulators, if the fundamental is suppressed. When limited by the fundamental, the harmonic powers reach the following saturated values [46,47]:

$$P_{n,F} = \eta_n \frac{P_{1,F}}{\sqrt{n}}\left(\frac{f_n}{n f_1}\right)^2. \tag{14}$$

Just as for the spontaneous UR, the spectral characteristics of the FEL radiation are therefore largely determined by the Bessel coefficients $f_{n;x,y}$, where all main effects are accounted for, while the corrections (13) in Equation (12) are influent if the respective losses are non negligible. The harmonic powers obtained with the above formula have proved to be in good agreement with the known documented data of all major FELs [31–38].

An alternative formulation of Huang and co-authors [52] for the FEL harmonic power in the nonlinear generation regime expresses the third harmonic power P_3, in terms of the inducing it fundamental P_1:

$$P_{Huang3} = \Theta\rho P_{beam}(P_1/(\rho P_{beam}))^3; \tag{15}$$

where the numerical coefficient has approximate value $\Theta \sim 10^{-1}$ and it is given by a triple integral in [52]. Evaluations of the authors of (15) in [52] and our estimations show that (15) predicts excessively high power of the third harmonic, higher than experimental by roughly one order of magnitude. Based on the measured data for many FELs, we propose the phenomenological correction to it as follows: $P^{corrected}_{Huang3} \approx 0.1 P_{Huang3}$. Then estimations for P_3 are in agreement with the data for many FELs. Estimates of the second harmonic power in [52] involve the beam section $\sigma_{x,y}$, the power of the near odd harmonic P_1 or P_3, and the bunching for the harmonics b_2 and b_1 or b_3. This yields the estimate

$$P_{Huang2} \approx P_n\left(\frac{\lambda_u k f_2}{\gamma 2\pi\sigma_{x,y} f_n}\frac{b_2}{b_n}\right)^2,\ n = 1.3. \tag{16}$$

Evidently, it is supposed that the harmonic powers and bunching values for the first and third harmonics are harmonized with each other so that the calculated result for the second harmonic should not depend much on whether we choose the first or third harmonic for reference in (16). In reality the predicted P_2 values may vary by more than one order of magnitude, dependent on whether we refer to $n = 1$ or $n = 3$ in (16). We phenomenologically correct the systematically lower than measured predictions of Huang by the factor 10 as follows: $P^{corrected}_{Huang2} \approx 10P_{Huang2}$. Then the predictions agree better with the measurements. Another formula for P_2 was derived by Geloni and coauthors in [53], where the second harmonic power P_2 is expressed in terms of the fundamental power P_1 and the Fresnel number $\Gamma = \Sigma/L_u\lambda_1$. The latter accounts for the difference in phases of the secondary waves at the wavelength λ_1, reaching the end of the undulator at the length L_u from the center and edges of the beam of the cross section Σ. We rewrite formula from [53] in the following explicit form:

$$P_{Geloni2} \approx P_1\frac{\Delta}{\Gamma}, \Delta = \frac{(K(J_0(K) - J_2(K)) + J_1(K))^2 + (J_1(K))^2}{(24\pi)^2 K(J_0(K/2) - J_1(K/2))^2}, \tag{17}$$

where $J_n(K)$ are the Bessel functions of the argument $K = k^2/\left(2\left(1 + k^2/2\right)\right)$ [53]. It should be noted that the conclusions of Huang and Geloni on the effect of the deflection angles are opposite each other: according to Huang, "the deflection angle increases the radiation of the 2nd harmonic", while according to Geloni, "the total power of the 2nd harmonic radiation does not depend on the deflection angles, or even can decrease due to the presence of deflection angles". In what follows we will apply and test both formulations of Huang and Geloni for the FELs we consider.

3. Spectral Analysis of the Radiation from the SPARC Undulators

Consider the radiation in the undulators of SPARC FEL [19,27]. Some data for the beam and the undulators of SPARC are collected in Table 1. We calculated the spontaneous radiation from SPARC both analytically and numerically with the SPECTRA program [54–57]. The SPARC UR spectrum consists of strong odd harmonics and weak even ones. This is common for the UR from an electron beam with quite small absolute emittance $\varepsilon_{x,y} \sim 9 \times 10^{-9}$ m $\times$ rad, small divergence $\theta_{div}\gamma \approx 0.02$ and low energy spread.

Table 1. Parameters of the beam and undulator of SPARC [19].

Electron Beam				Undulator	
Parameter	**Value**	**Parameter**	**Value**	**Parameter**	**Value**
I_0, A	53	σ_e, %	0.05–0.1	λ_u, cm	2.8
E, MeV	152	β_x, m	1.5	L_u, m	2.1
$\gamma\epsilon_x$, m $\times$ rad	2.9×10^{-6}	β_y, m	1.5	N	75
$\gamma\epsilon_y$, m $\times$ rad	2.5×10^{-6}	*radius*, µm	120	k	2.07
				k_{Eff}	2.07

3.1. The Effect of the Energy Spread

Analytical results for the harmonic intensities, obtained with (6) and (8), are undistinguishable from each other; we present one of each for the spread σ_e = 0.1% and for σ_e = 0.05% in Figure 1; they are in good agreement with numerical results, obtained with SPECTRA code and shown in Figure 2. The effect of the energy spread on the harmonic radiation is evidently detrimental. The comparison of the spectrum for the energy spread σ_e = 0.05% with the spectrum for larger spread σ_e = 0.1% (Figure 1a vs. Figures 1b and 2a vs. Figure 2b) shows expectedly weaker high harmonics for higher energy spread. The higher the number of the harmonic, the more the losses caused by the energy spread; the fundamental is less affected than other harmonics. Note that higher absolute values and different shape of the envelope of the spectrum for σ_e = 0.05% as compared with that for σ_e = 0.1%. Lower energy spread, σ_e < 0.05%, does not significantly modify the spectrum.

High energy spread in a beam not only cuts off the harmonics, but prevents efficient bunching in FELs, where the condition $\sigma_e \bigcirc \rho_n/2$ determines the stable bunching at the n-th harmonic wavelength. Since the Pierce parameter ρ is of the order of magnitude of ~10^{-3}–10^{-4}, a beam with high energy spread is not unsuitable for modern insertion devices in UV- and X-ray range, where close to monoenergetic beams are needed to generate coherent radiation.

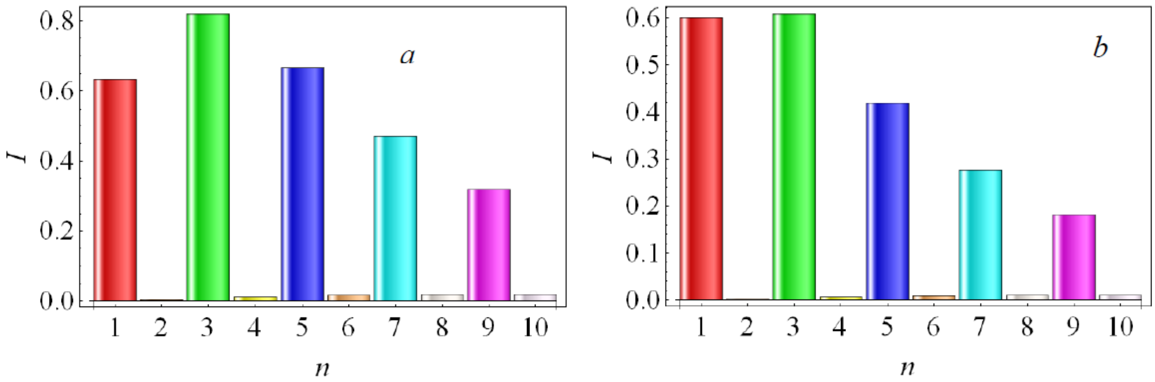

Figure 1. Analytically computed spontaneous SPARC UR spectrum for $\gamma\varepsilon$ = 2.8 µrad × m and the beam energy spread: (**a**) σ_e = 0.05%, (**b**) σ_e = 0.1%.

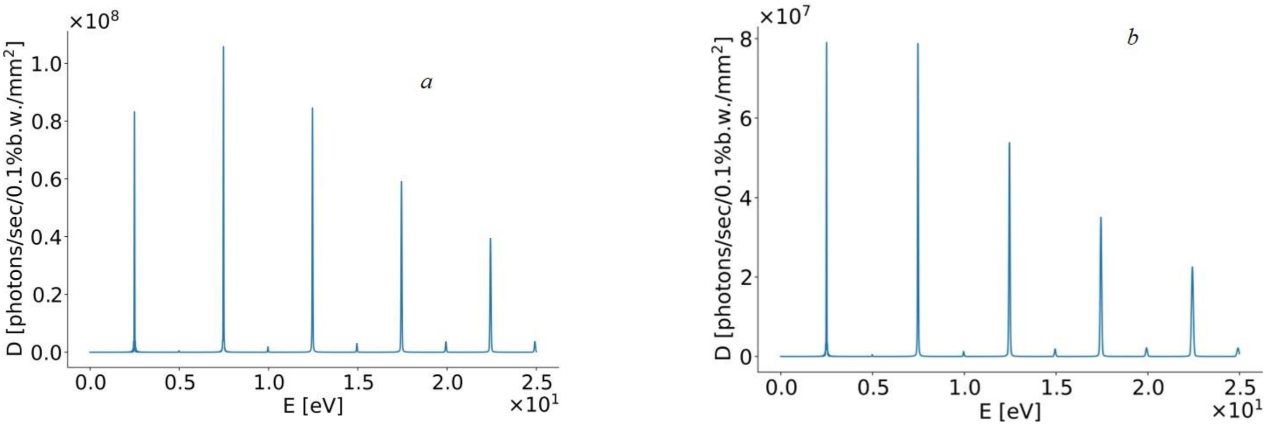

Figure 2. Numerical SPECTRA simulation of SPARC UR spectrum for $\gamma\varepsilon_{x,y}$ = 2.8 µrad × m and the beam energy spread: (**a**) σ_e = 0.05%, (**b**) σ_e = 0.1%.

3.2. The Effect of the Asymmetry of the Beam

Here we analyze the effect of the divergence and asymmetry of an electron beam on the UR spectrum of the planar undulator. Indeed, the planar undulator distinguishes the direction across its field, where almost the whole power radiation is polarized. Real electron beam has finite size; this causes a weak component of radiation with the polarization in the plane, containing the undulator field, differently from the ideal case, when all the radiation is polarized across the undulator field. Moreover, the finite size of the beam induces even harmonics on the undulator axis and not only off the axis. Asymmetry of the beam affects both UR polarizations. The emittance along the undulator field causes even harmonics polarized across this field and vice versa. The comprehensive result for the harmonic power, however, does not depend significantly on the asymmetry of the beam. We considered the examples for the SPARC with the beam emittances $\gamma\varepsilon$ = 2.2 µrad × m and $\gamma\varepsilon$ = 3.4 µrad × m. We interchanged the parameters of the beam for the axes $x \leftrightarrow y$ and showed the proper spectrum in Figures 3 and 4, distinguishing the polarizations. The finite size of the beam causes even harmonics and the asymmetry of the beam evidently affects polarizations of the UR. Note in Figures 3b and 4b as the interchange of the asymmetry of the beam practically does not affect odd harmonics, radiated with the polarization across the plane of the planar undulator field. On the contrary, the beam asymmetry affects even harmonics in the same plane, as seen in Figures 3a and 4a. The difference in the intensities of the even harmonics is roughly 1.5 times which matches the degree of the asymmetry: the ratio of the emittances is ~1.5 times. The average value of the emittance matters fir the total harmonic power, so that the results for the symmetric beam with the emittance $\gamma\varepsilon_{x,y}$ = 2.8 µrad×m, shown in Figures 1b and 2b, are very close to the total harmonic power from the asymmetric beam, no matter along which axis the emittances is greater and lower. The sum of the two polarizations for the even harmonics in Figure 3a,b is the same as the sum of the harmonic powers in Figure 4a,b and it is nearly identical to that shown in Figure 2b for the symmetric beam with average emittance $\gamma\varepsilon_{x,y}$ = 2.8 µrad × m.

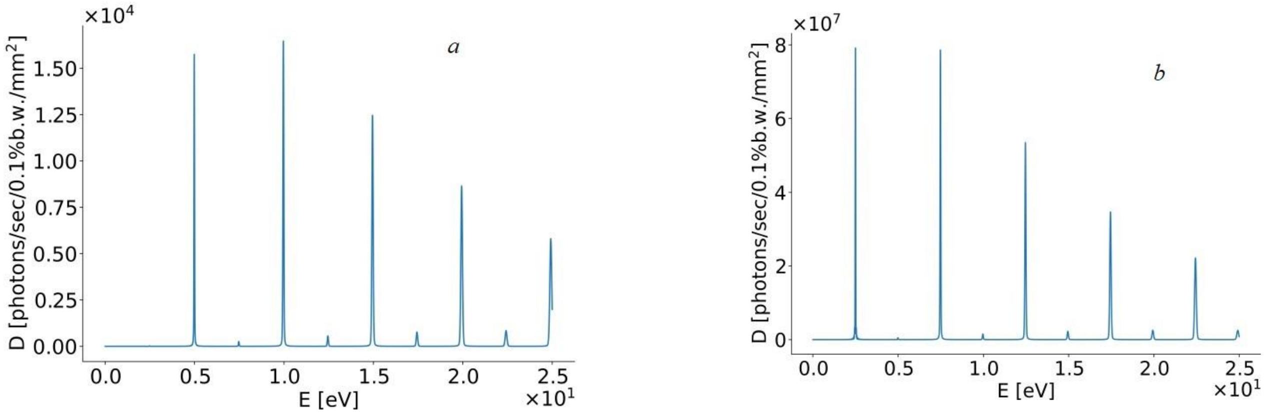

Figure 3. Numerical SPECTRA simulation of the UR spectrum from SPARC for σ_e = 0.1%, $\gamma\varepsilon_x$ = 2.2 µrad × m and $\gamma\varepsilon_x$ = 3.4 µrad × m: (**a**) x-polarisation (**b**) y-polarization.

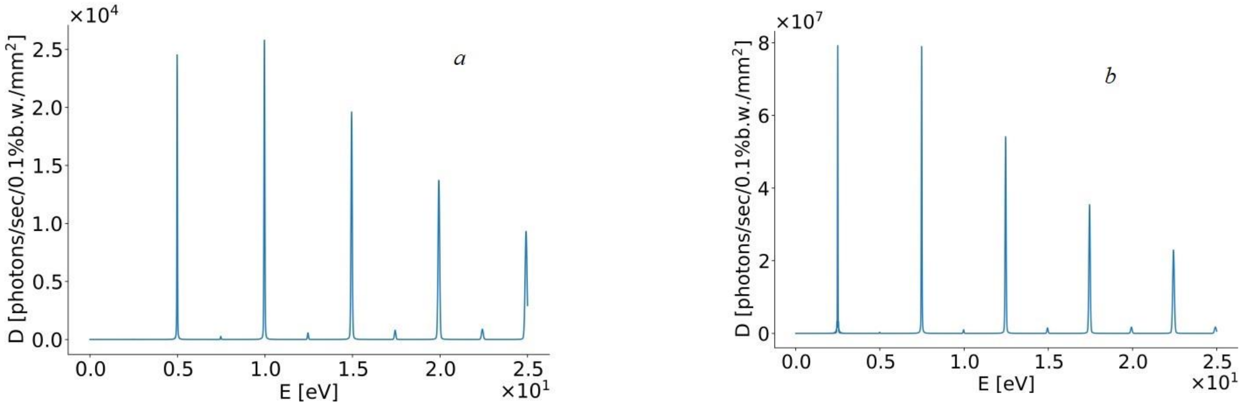

Figure 4. Numerical SPECTRA simulation of the UR spectrum from SPARC for σ_e = 0.1%, $\gamma\varepsilon_x$ = 3.4 µrad × m and $\gamma\varepsilon_y$ = 2.2 µrad × m: (**a**) x-polarization, (**b**) y-polarization.

These results are in line with our earlier theoretical results in [43], where the analytical calculations with generalized forms of Airy-type functions accounted for the non-periodic two-component magnetic field across the undulator axis in both directions along and across the field. Here we formulate the result, which follows from [43] and consists in that weak non-periodic magnetic component, ~0.01% of the undulator field, deviates the electrons off the undulator axis and disrupts the coherence of the electron oscillations along the undulator, if the latter is few meters long, the effect can be noticeable. In this case, the total power of the even harmonics, induced by the off-axis effects, depends on the degree of the deviation of the beam off the axis, but not on the specific direction of the beam deviation across the undulator axis. The asymmetry is determined by the distinguished direction of the planar undulator field and the direction of the beam deviation off the axis.

3.3. The Analysis of the FEL Harmonics in SPARC

Differently from the spontaneous radiation, the spectrum of a single-pass FEL is usually limited to few harmonics; this is due to the nature of the FEL radiation, where the electrons in the bunch interact with the electromagnetic wave of the radiation and the bunching occurs at the harmonic wavelengths, which ensures their coherent radiation. The evolution of FEL harmonics along SPARC undulators is shown in Figure 5; we show the power evolution for the first three harmonics, n = 1,2,3, although fifth harmonic is allowed by the conditions on the beam emittance: $\varepsilon_{x,y} \sim \lambda_5/4\pi$ fulfilled and the energy spread of the beam is as low as the Pierce parameter for the fifth harmonic, $\sigma_e \approx \rho_5$, so the bunching at its wavelength is possible. To demonstrate the effect of the energy spread we modeled FEL harmonic powers for $\sigma_e = 0.1\%$ and $\sigma_e = 0.05\%$ as shown respectively in Figure 5a,b. The saturation was not achieved in the experiment and the measurements after the last undulator are at $\approx$12.5 m of pure undulator length. We calculated the gain length $L_g \approx 0.65$ m and the saturation is expected after $L_g \approx 13$ m of undulator length.

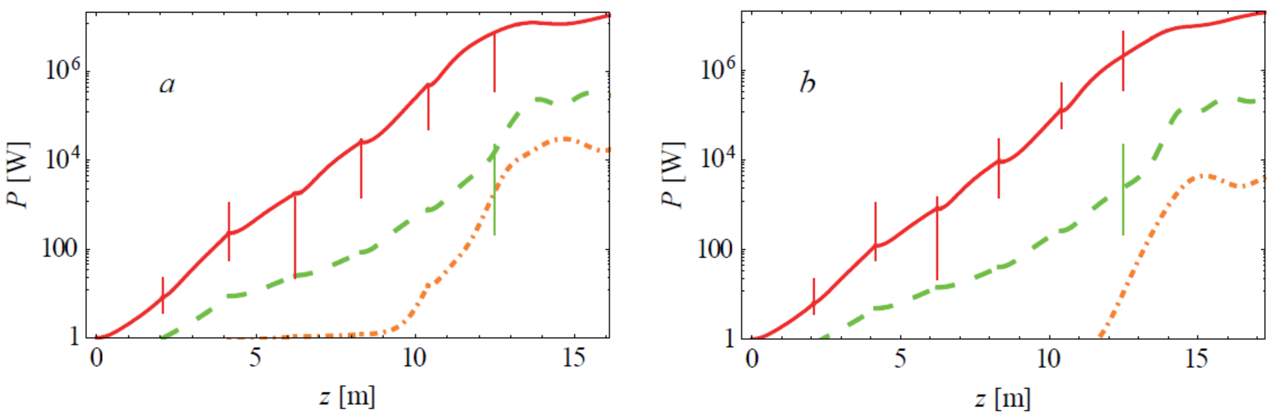

Figure 5. (**a**) Harmonic power evolution along SPARC undulators, λ_1 = 498 nm. (**a**) $\sigma_e = 0.05\%$ (**b**) $\sigma_e = 0.1\%$. Harmonics are denoted by coloured lines: n = 1—red solid, n = 2—orange dash-dotted, n = 3—green dashed, interval of measured values is shown by the vertical lines.

Only the fundamental tone and the third harmonic were measured; the measurements are shown by the intervals of the values after each undulator section, following the reports in [19]. The saturation was not achieved in the SPARC experiment and maximum pulse energy $E_\gamma \approx 0.01$ mJ was collected after the sixth undulator close to saturation. For the reported bunch length $\tau_e \approx 2.5$ ps we estimate photon pulse time $\tau_\gamma \cong \sqrt{2\pi}\tau_e\sqrt{L_g/L_s} \approx$ 1.5 ps and this yields the FEL power for the collected energy E_γ $P_{\max} \approx 7.2 \times 10^7$ W. This value matches our result for the energy spread $\sigma_e = 0.05\%$ exactly.

Various numerical programs were used by the authors of this FEL experiment to simulate their FEL [19,27]. They gave predictions with the discrepancy of about one order of magnitude for the fundamental and up to two orders of magnitude for the third harmonic. Our theoretical results are at the high end of the measured values for the maximum tuning of the FEL and within the range of the numerical simulations, reported in [19,27]. We calculated the amplification factor for SPARC FEL ~10^7 and the following harmonic content: ~0.15% for the second, ~1% for the third and ~0.08% for the fifth harmonic (the latter is not shown in Figure 5).

Following the theoretical approach of Huang et al. as proposed in [52], we get the third harmonic power prediction one order of magnitude higher than that measured. With our phenomenological correction Θ in (15), we get the right result ~1%. For the second harmonic, following [52], and using correction factor of ten in (16), we get, dependently on that first or third harmonics are used for reference in (16), the content of the second harmonic $P_2/P_1 \approx 0.04$–0.2%, in accordance with our result ~0.15%. Using the theory from [53], we get the second harmonic power one order of magnitude higher than in Figure 5. Our analytical calculation accounts for the effective angle of the photon-electron interactions, $\gamma\overline{\theta} \approx 0.06$, which is three times the divergence angle, $\theta_{div}\gamma \approx 0.02$, and this yields correct values for the FEL parameters, such as the gain L_g, the saturation L_s, and the harmonic powers. This confirms the validity of our approach, also verified in earlier publications with other FEL experiments. For the second harmonic, our theoretical result agrees with the results of Huang; for the fifth harmonic we get P_5~$0.1P_3$, which is expected, though not reported, despite the fifth harmonic is being allowed: $\varepsilon_{x,y}$~$\lambda_5/4\pi$ and $\sigma_e \approx \rho_5$. The measured radiation spectral density was 0.35% [19]. Our analytical estimation of the spectral width with the Bessel coefficients (3) is in agreement with the experiment. The usual estimate for SASE is $\Delta\lambda/\lambda \cong \sqrt{\rho_1/(L_s/\lambda_u)} \approx 0.2\%$, and it is about of half of the measured width value.

4. Spectral Analysis of the Spontaneous and Stimulated UR at LEUTL

At LEUTL FEL [17,18], the radiation wavelength λ_1~530 nm is close to that at SPARC FEL. However, the parameters of the installation are somewhat different: the beam section, $\sigma_{x,y}$ = 0.25 mm, is twice as wide as that at SPARC; the divergence, $\theta_{div} \approx 0.17$ mrad, $\gamma\theta_{div} \approx 0.085$, is four times larger than at SPARC, the smallest measured emittance, $\gamma\varepsilon_{\mathrm{x,y}}$~6 $\times$ 10^{-8} m $\times$ rad, is seven times larger than at SPARC. Thus, the main difference between LEUTL and SPARC is in the beam emittance, which is much larger at LEUTL. Some data for the beam and undulators of LEUTL are given in Table 2.

Table 2. Parameters of the beam and undulator of LEUTL [18].

Electron Beam				Undulator	
Parameter	**Value**	**Parameter**	**Value**	**Parameter**	**Value**
I_0, A	210	σ_e, %	0.1	λ_u, cm	3.3
E, MeV	217	β_x, m	1.5	L_{u}, m	2.4
$\gamma\epsilon_x$, m $\times$ rad	$5.9\pi \times 10^{-6}$	β_y, m	1.5	N	72
$\gamma\epsilon_y$, m $\times$ rad	$6.4\pi \times 10^{-6}$	*radius*, µm	430	k	3.1
				k_{Eff}	3.1

Considering the given characteristics of the LEUTL beam, the betatron effects may contribute in it to the harmonic radiation from LEUTL undulators. We have studied the case carefully and accounted for the betatron effects and large emittance by taking the convolution (8) with the Bessel coefficients (3), where the contributions from betatron oscillations are distinguished; we compared the result with that we obtained with the simple energy spread convolution (6). The analytical spectrum of the spontaneous UR from LEUTL is shown in Figure 6. Note that the rate of even harmonics in LEUTL is significant, contrary to the spectrum of SPARC. This is mainly due to the angular effects, rather than to the betatron oscillations; the latter contribute less than a quarter to the total intensities, while three quarters and more for high harmonics come from the angular effects. The Bessel coefficients for the harmonics $n = 1, \ldots, 10$ read as follows: f_n = {0.753, 0.073, 0.334, 0.077, 0.218, 0.078, 0.158, 0.078, 0.119, 0.076}. The betatron contributions to the odd harmonics are absolutely negligible. For even harmonics n = 2,4,6,8,10 the betatron terms of the Bessel coefficients read as follows: $f_{2,4,6,8,10\ beta}$ = {0.019, 0.014, 0.011,0.009, 0.008}. They produce some effect on the intensities of even harmonics, but the difference in figures can be barely noticed and we omit them for brevity.

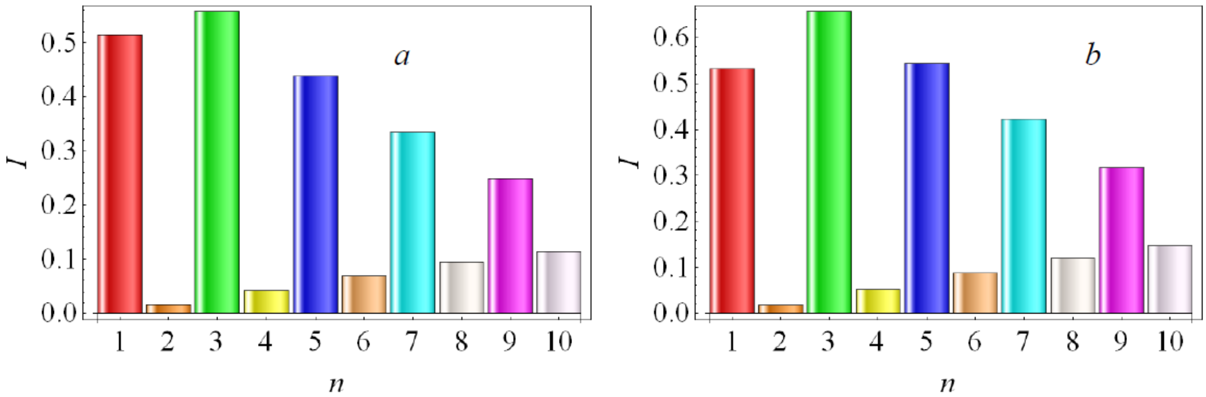

Figure 6. Analytically computed LEUTL spontaneous UR spectrum, $\gamma\varepsilon$ = 6.2 µrad × m: (**a**)—with comprehensive energy spread and angle convolution (8), (**b**)—with common energy spread convolution (6).

The account for the energy spread and angular effects on the UR is done with the comprehensive convolution (8) and the resulting spectrum is shown in Figure 6a. The UR spectrum that accounts only for the energy spread is computed with the common convolution (6) and is shown in Figure 6b. The emittance of LEUTL beam is significant and the associated angular effects spread the radiation lines to a kind of Airy-type function, different from the ideal sinc-type function. This affects high harmonics more than low ones and for the considered LEUTL it makes a difference: when counting with (8), the fifth harmonic is weaker than the fundamental contrary to that when counting with (6), when the fifth harmonic is stronger than the fundamental. Note, that for SPARC the results obtained with (8) vs. (6) were the same.

Complex numerical simulation with SPECTRA code yields upon numerical solution of the set of equations for charges, the spectrum of LEUTL spontaneous UR in Figure 7. Note, that the spectrum in Figure 7 is closer to that in Figure 6a, obtained with comprehensive convolution (8); The result of simple energy spread convolution (6) in Figure 6b agrees less well with the accurate numerical result of SPECTRA in Figure 7.

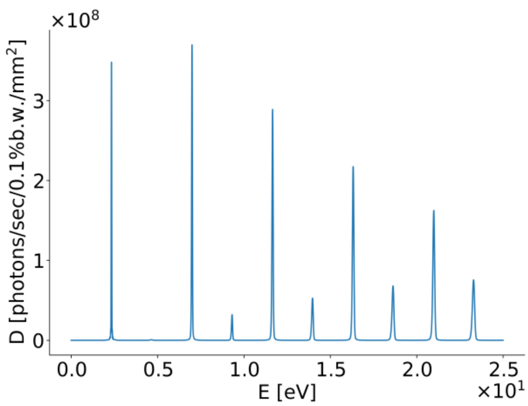

Figure 7. LEUTL spontaneous UR spectrum: numerical result of SPECTRA.

We estimated the split of the radiation line that was due to the betatron oscillations in the beam and found the distance between betatron harmonics within the UR line $\delta\lambda \cong k\lambda/n\sqrt{2}\gamma\big|_{n=1} \cong 2.7$ nm. For the Bessel function $\widetilde{J}_p$ (4), describing the betatron split, we found for the betatron harmonics $p = -3, \ldots, 3$ the values $\widetilde{J}_p$ = {0.00, 0.08, 0.47, 0.75, 0.43, 0.16, 0.04}. The main contribution thus comes from $p = -1,0,1$. Then we get the split width $\Delta \approx 5.5$ nm for the radiation wavelength λ_1 = 532 nm. This yields the spectral density

$\Delta/\lambda \approx 0.01$, comparable with the natural line width at its half-height: $0.9/N = 0.0125$ for the undulator of 72 periods at LEUTL.

Among many FEL experiments at LEUTL, we consider that where the most complete set of measurements for the radiation was performed and documented in [18] (see some data in Table 2). The fundamental and the second harmonics were carefully measured along the undulators [18]; experimental values are shown in Figure 8a by colored dots; the domain 1–2% for the third harmonic is shown by the green area after 16 m. Our theoretical results for the harmonic evolution are shown by the colored lines. Importantly, when computing the FEL harmonic powers, we must account not only for the emittance and betatron effects, but also for the effective angles of the electron-photon interaction in the beam. Otherwise the calculated second harmonic power is significantly lower than that measured. This was underlined in our earlier publications [32–36].

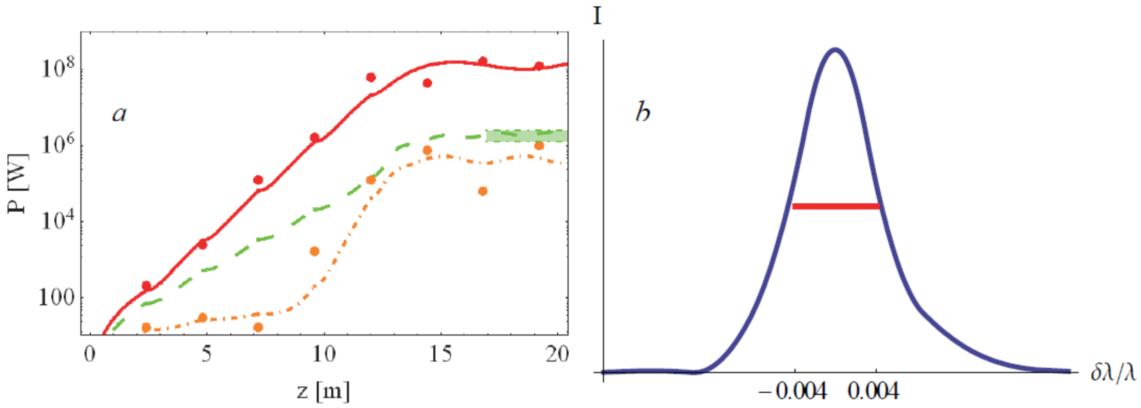

Figure 8. (**a**) Harmonic power evolution along LEUTL undulators, λ_1 = 540 nm; the harmonics are denoted by colored lines: n = 1—red solid, n = 2—orange dash-dotted, n = 3—green dashed, experimental range for the third harmonic content, 1–2%, is shown by the green area, experimental values for the second and fundamental are shown by colored dots, following the reports in [18]; (**b**) radiation spectral density: theoretical calculation—blue line, measured bandwidth—red line.

We also estimated the harmonic powers using the theory of Huang [52] without corrections and using the theory of Geloni [53]. Following Huang with our corrections, we get for the third harmonic the estimate P_3~1 MW, matching our prediction and the measured range denoted by the green zone in Figure 8a. For the second harmonic power, following Huang with our corrections, dependently on whether we refer to the third or first harmonic power, we respectively get the range P_2~100–600 kW, which is within the experimental range of values, denoted by the orange dots after 15 m. Estimate for the second harmonic power, using the approach of Geloni yields the value P_2~350 kW, in the middle of the experimental range of saturated powers of the second harmonic. Our own theoretical result is obtained accounting for the effective angle $\overline{\theta}$ of interactions of the electrons with radiation in the undulator on one gain length L_{gain} = 0.75 m: $\overline{\theta} \approx \sigma_{x,y}/L_{gain}$ $\approx$ 0.28 mrad, $\gamma\overline{\theta} \approx 0.12$. This angle exceeds, but not greatly, the divergence at LEUTL: $\gamma\theta_{div} \approx 0.07$. Accounting for $\overline{\theta}$, we obtain the following Bessel coefficients for the first five harmonics: $f_{n=1,2,3,4,5} \approx \{0.75, 0.14, 0.31, 0.15, 0.18\}$ and the resulting harmonic power evolution nicely agrees with the measurements in both linear and nonlinear generation regimes (see Figure 8a). Otherwise, accounting only for emittances and betatron oscillations, we get the theoretical value for the power of the second harmonic one order of magnitude lower than that measured. For even harmonics we distinguish analytically and compute the Bessel factor terms, associated with betatron effects; they are small and comparable with the terms in y-polarization because of the angular effects (see (3)): $f^{\beta}_{n=2,p} \sim f_{n=2,y} \approx 0.02$; we get larger contribution in x-polarization from the electron-photon interaction angle $\overline{\theta}$; the relation is as follows: $f_{n=2,x} \approx 0.14 >> f_{n=2,y} \sim f^{\beta}_{n=2,p} \approx 0.02$. Our theoretical curves nicely lay between the measured values. The calculated gain L_g = 0.75 m and saturation L_s = 16 m lengths agree with the experiment report in [18].

Estimates from the original Huang work [52] without our correction for the third harmonic appears one order of magnitude higher than the measured P_3; for the second harmonic the original theory [52] predicts one order of magnitude lower values than the measured P_2. The estimate for P_2 from Geloni [53] is within the range of the measured values between the orange dots after 16 m in Figure 8a.

Note, that the conditions $\varepsilon_{x,y} \leq \lambda_0/4\pi, \sigma_e \leq \rho/2$ are fully satisfied only for the fundamental; for the harmonics they are just weakly satisfied: $\varepsilon_{x,y} \sim \lambda_{2,3}/4\pi$ and $\sigma_e \approx \rho_2 \approx 0.7\rho_3$. We also estimated spectral density of the radiation at LEUTL; accounting for $p = \{0, \pm 1\}$ in (3), which gives the main contribution, we obtain spectral density $\delta\lambda/\lambda \sim 0.8\%$, in agreement with the reports in [18]; proper measured result is shown by the red line in Figure 8b, while our theoretical estimate is shown by the blue line in Figure 8b.

5. Spectral Analysis of the Spontaneous and Stimulated UR at LCLS

In this section we address the spontaneous and stimulated radiation properties of the first ever built and arguably best documented X-ray FEL, LCLS [15,16]. It has undulators with fixed deflection parameter k = 3.5 and it generates radiation at 1.5 nm and 0.15 nm for two different energies of the beam. Some data on the LCLS beam and undulators are collected in Table 3.

Table 3. Parameters of the beam and undulator of FEL LCLS.

Electron Beam				Undulator	
Parameter	**Value**	**Parameter**	**Value**	**Parameter**	**Value**
γ-factor	8400	I_0, kA	1	λ_u, cm	3
$\gamma\varepsilon_{x,y}$, μm × rad	0.4	$\beta_{x,y}$, m	10	L, m	3.4
$\sigma_{x,y}$, μm	~23	σ_e, %	0.03	N	113
γ-factor	26,600	I_0, kA	3.5	k	3.5
$\gamma\varepsilon_{x,y}$, μm × rad	0.4	$\beta_{x,y}$, m	25	k_{eff}	3.5
$\sigma_{x,y}$, μm	~30	σ_e, %	0.01		

The spontaneous UR spectrum of LCLS undulators displays a long array of odd harmonics, while even harmonics are minor even at angles close to divergence as shown in Figure 9a; our numerical simulations with SPECTRA yield the result, shown in Figure 9b. Low content of even harmonics is due to low emittance of the beam and high content of higher odd harmonic is due to large value of the deflection parameter k and low losses.

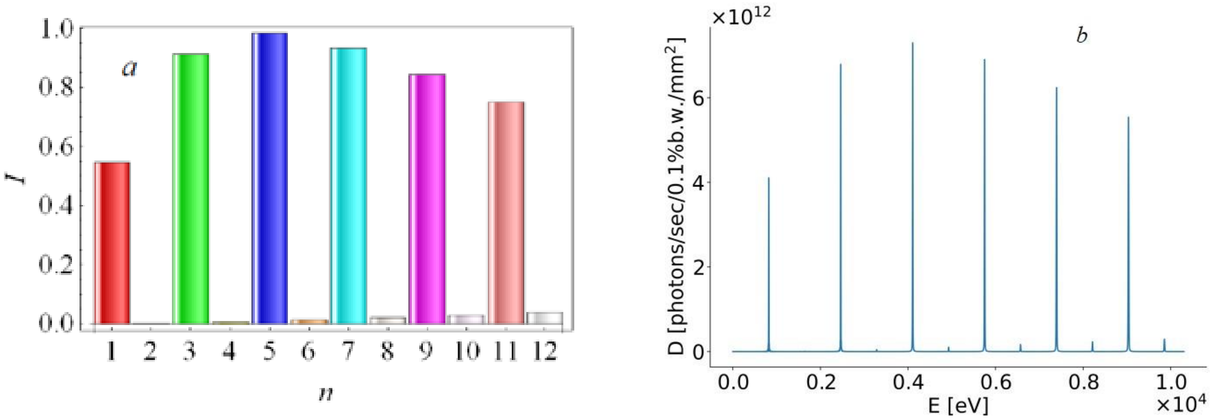

Figure 9. Spontaneous UR spectrum LCLS on the axis: (**a**)—analytical, (**b**)—numerical SPECTRA.

Regarding the contribution from betatron oscillations, the proper Bessel factor, for example, for the second harmonic reads f_2^{beta}~0.002; however, the total value of the Bessel coefficients for the harmonics n = 2,4,6 is one order of magnitude larger: $f_{2,4,6}$~0.02. The effect of the betatron oscillations on the spectrum is minor if not negligible; it can-not be distinguished by the naked eye in figures and we omit proper plots. The radiation line splits in betatron harmonics that are due to the betatron oscillations. In the low emittance beam of LCLS, the main contribution comes from $p = -2, \ldots, 2$; the betatron harmonics in the split are distant by $\delta\lambda \cong k\lambda/n\sqrt{2}\gamma\Big|_{n=1} \cong 0.45$ pm from each other. The total split width is therefore $\Delta \approx 1.8$ pm and proper spectral density $\Delta/\lambda \approx 0.1\%$; this is much less than the natural UR line width of the LCLS undulator with N = 113 periods: $0.9/N = 0.8\%$. Thus, the betatron split width is well within the radiation line width.

The LCLS FEL experiments [15,16], have been explored theoretically in a long array of studies in the preceding publications [23–39]. We briefly outline the theoretical predictions of our formalism and the predictions, based on the corrected formulae by Huang and Geloni for the harmonic powers for the FEL radiation from beam with the energy E = 4.3 GeV. Our results are demonstrated in Figure 10 together with the experimentally measured saturated harmonic powers [15,16].

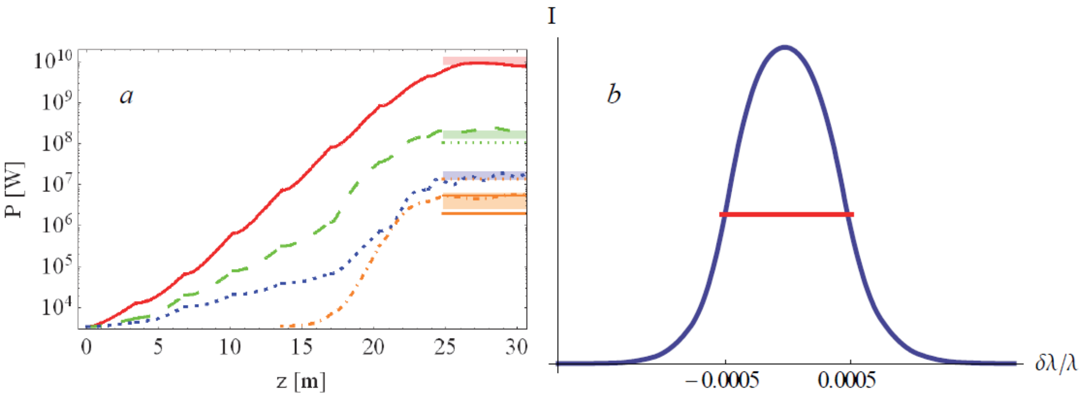

Figure 10. (**a**) The harmonic power evolution along the undulators in LCLS FEL, λ_1 = 1.5 nm. The harmonics are denoted by colored lines: n = 1—red solid, n = 2—orange dashdotted, n = 3—green dashed, n = 5—blue dotted. The reported harmonic power range [16] is shown by the colored areas. Estimations for the 2nd harmonic powers are denoted by the orange lines: by Huang with our correction—solid thick and thin orange lines, by Geloni—dotted orange line. Estimate for the third harmonic power by Huang with our correction—dashed green line. (**b**) Radiation spectral density: theoretical calculation—blue line, design bandwidth—red line.

The measured third harmonic content was ≈2% (green line and area in Figure 10); occasional drop off to 0.2% because of poor FEL performance on the day of the measurement is omitted here. The content of the fifth harmonic was estimated at the experimental station at ~1/10 of the third harmonic content, i.e., ~0.2%. The proper area and theoretical result are denoted in blue in Figure 10. The measured second harmonic content was ~0.04–0.1% and is shown by the orange area in Figure 10. Our theoretical result for the second harmonic power is denoted by the orange dotdashed line; it is in the orange area of measured saturated power values. The collected FEL pulse energy in the experiment was E_γ = 1 mJ; for the reported electron bunch length τ_e = 0.2 ps we get the power ≈ 7 GW. The average reported saturated energy in all experiments was 1–2 mJ for the photon pulses of ~100–300 fs; this yields similar average power: 7.5 GW and the experimental range is denoted by the red area in the saturation domain after 26 m. Our result also fits these measurements. For the third and the fifth harmonic powers we obtain theoretical values also laying within the experimental range. Predictions for the third harmonic by Huang with our correction are close to the experimental result. For the second harmonic original theory of Huang predicts, as usual, one order of magnitude lower power than measured; however, the corrected formula of Huang yields right result. The theory of Geloni (17) predicts second harmonic some stronger than experimental at LCLS in soft X-ray band.

The design spectral density for LCLS radiation was ~0.1%; our calculations agree with it as shown in Figure 10b. The estimate for SASE also yields $\Delta\lambda/\lambda \cong \sqrt{\rho_1/(L_s/\lambda_u)} \approx$ 0.1%. In real device the performance was sometimes less good and the measured values varied: ~0.1–0.5%.

6. Conclusions

In this work we addressed the spectral properties of the radiation from some FEL undulators and beams and explored the effect of the beam parameters and beam symmetry on the spectrum and on the radiation of harmonics. Special attention was paid to the effect of the symmetry and divergence of the beam on the radiation properties. For two FELs SPARC and LEUTL both radiating at λ~500 nm, and their proper undulators and beams with similar energies and energy spread, but different emittances, we compared the spontaneous and single-pass FEL radiation. At the end we considered the LCLS FEL X-ray radiation. In our analytical technique we used the generalized forms of Bessel and Airy-type functions to account for all main factors affecting the radiation. We computed the common convolution with the Gaussian energy spread distribution and the advanced convolution with generalized Airy-type function to account for the shape and asymmetry of the spectral line of the spontaneous UR in beams with large emittances. We especially compared the spectrum for asymmetric beams and explored the effect of the beam axial asymmetry on the UR spectrum. Numerical studies with SPECTRA program were done for that purpose. Spectra simulations also confirmed our other analytical results for the effect of the energy spread etc. We also studied FEL harmonic powers using several different theoretical approaches, developed by different authors, and applied them to SPARC, LEUTL and LCLS.

Our theoretical analysis fully agrees with the existing data for SPARC, LEUTL and LCLS.

For the spontaneous UR we found that the asymmetry of the beam and its deviation off the axis in one plane expectedly causes asymmetry in the radiation pattern in the normal plane. We considered the UR in the case of the break of the symmetry that was due to the distinguished direction of the field of a planar undulator and of the definite asymmetry of the beam imposed by its different from each other emittances. This appeared to have no effect on the resulting harmonic powers. The latter depend on the degree of the beam deviation off the axis and the direction does not matter. Similarly, the asymmetry of the beam caused by different emittances in the directions across the axis itself does not affect the total harmonic power, but effects the distribution of the harmonic power in polarizations. The total harmonic power, however, senses the average emittance and divergence and is not affected by the asymmetry of the beam, provided the average vale of emittance is preserved.

Large emittance of the beam, such as at LEUTL, may increase even harmonic radiation on the axis but the asymmetry of the beam sections does not matter for the harmonic power. Spontaneous radiation of LEUTL presents a high rate of even harmonics in the direction of divergence, while their rate is minor on the axis. At the same time relatively large angular contributions asymmetrically broaden the radiation line, so that the account for the energy spread alone with typical symmetric Gaussian convolution did not match the numerical results of SPECTRA. We had to account analytically for the change of the UR line shape from symmetric sinc function to the asymmetric Airy-type generalized function. The convolution with the latter yielded the spectrum in agreement with the numerically simulated by SPECTRA program. The change of the harmonic powers, described by the Airy-type function, reached ~30–50% as compared with the common symmetric sinc function. Contrary to LEUTL, the SPARC and LCLS undulators with their proper beams radiate weak even harmonics because of small emittances.

For the FEL radiation we confirm the detrimental effect of the energy spread on the harmonic in particular, but for the range of the spread σ_e~0.05–0.1% simulations matched the experimental range of values for the FEL powers along the undulators. Even harmonics in the FEL radiation appear because of the effective angles of photon–electron interaction in the beam and they do not sense the asymmetry of the beam. Off the axis beam deflection may affect FEL harmonic powers, but the direction of the deflection has no effect. In LCLS the beam deflection may be comparable with the effective angle of electron-photon interaction in a very narrow beam; the second harmonic in LCLS ~0.04–0.1% is due to both angles. LEUTL FEL has quite high second harmonic content ~0.5% because of the wide beam and large effective angle. SPARC second harmonic content ~0.1% is also explained by the effective angles of photon–electron interaction, while the emittance is small. The third harmonic in all three FELs has ~1% content. A fifth harmonic is possible in LCLS and SPARC, while in LEUTL it is limited by large beam divergences. The results agree with known measured values for all three FELs.

The estimates with the original theory from [52] for the FEL harmonic powers yield a too strong third harmonic and a too weak second harmonic. We have introduced phenomenological corrections, which restore agreement with experiments for the formalism of Huang [52]. We confirm the conclusions of Huang et al. that the second FEL harmonic power depends on the off-axis angles in particular, on the deflection angle and it increases if they rise; however, we specify that for a FEL the angle of photon–electron interaction in the undulator on the gain length usually exceeds the deflection angles and it plays a role rather than other angular effects. The theory from [53] gives reasonable estimates for the second FEL harmonic powers except for SPARC, where the prediction appears too high. The conclusion of Geloni et al. that off-axis deflection has no effect on the even harmonics is contradictory. It is true in the sense that the even harmonics in a FEL originate mainly from the angles of electron-photon interaction and not from the beam deflection. However, even harmonics originate from the angular effects, as we have analytically demonstrated, and if the deflection is comparable with the electron–photon interaction angles, then both of them matter like in LCLS undulators.

The proposed analytical technique gives correct and accurate estimates for the harmonic content in undulator radiation even in the cases when the beam is far from ideal, in the presence of noticeable angular and betatron effects, distorting the radiation lines. The betatron effects, as we have demonstrated analytically, have minor effect for harmonic powers, but they may split the radiation lines noticeably. Our approach can be applied to any other FEL for theoretical analysis of its UR and FEL radiation and study of possible effects of the beam parameters on the harmonic radiation. This may be used in both operating FELs and in the installations under upgrade or being built.

Author Contributions: Conceptualization, K.Z.; Data curation, I.F.; Software, I.F.; Validation, I.F.; Writing—original draft, K.Z. All authors have read and agreed to the published version of the manuscript.

Funding: This research received no external funding.

Institutional Review Board Statement: Not applicable.

Informed Consent Statement: Not applicable.

Data Availability Statement: Not applicable.

Conflicts of Interest: The authors declare no conflict of interest.

References

1. Motz, H.; Thon, W.; Whitehurst, R.N.J. Experiments on Radiation by Fast Electron Beams. *Appl. Phys.* **1953**, *24*, 826. [CrossRef]
2. Ginzburg, V.L. On the radiation of microradiowaves and their absorbtion in the air. *Isvestia Akademii Nauk SSSR (Fizika)* **1947**, *11*, 1651.
3. Madey, J.M. Stimulated Emission of Bremsstrahlung in a Periodic Magnetic Field. *J. Appl. Phys.* **1971**, *42*, 1906. [CrossRef]
4. McNeil, B.W.J.; Thompson, N.R. X-ray free-electron lasers. *Nat. Photonics* **2010**, *4*, 814. [CrossRef]
5. Pellegrini, C.; Marinelli, A.; Reiche, S. The physics of X-ray free-electron lasers. *Rev. Mod. Phys.* **2016**, *88*, 015006. [CrossRef]
6. Schmüser, P.; Dohlus, M.; Rossbach, J.; Behrens, C. Free-Electron Lasers in the Ultraviolet and X-Ray Regime. In *Springer Tracts in Modern Physics*; Springer International Publishing: Cham, Switzerland, 2014.

7. Huang, Z.; Kim, K.J. Review of X-ray free-electron laser theory. *Phys. Rev. ST-AB* **2007**, *10*, 034801. [CrossRef]
8. Margaritondo, G.; Ribic, P.R.J. A simplified description of X-ray free-electron lasers. *Synchrotron Rad.* **2011**, *18*, 101. [CrossRef]
9. Saldin, E.L.; Schneidmiller, E.A.; Yurkov, M.V. *The Physics of Free Electron Lasers*; Springer: Berlin/Heidelberg, Germany, 2000.
10. Bonifacio, R.; Pellegrini, C.; Narducci, L. Collective instabilities and high-gain regime free electron laser. *Opt. Commun.* **1984**, *50*, 373. [CrossRef]
11. Margaritondo, G. Synchrotron light: A success story over six decades. *Rivista del Nuovo Cimento* **2017**, *40*, 411.
12. Bagrov, V.G.; Bisnovaty-Kogan, G.S.; Bordovitsyn, V.A.; Borisov, A.V.; Dorofeev, O.F.; Ya Epp, V.; Pivovarov, Y.L.; Shorokhov, O.V.; Zhukovsky, V.C. *Synchrotron Radiation Theory and Its Development Ed v a Bordovitsyn*; Word Scientific: Singapore, 1999; p. 447.
13. Ternov, I.M.; Mikhailin, V.V.; Khalilov, V.R. *Synchrotron Radiation and Its Applications*; CRC Press: Boca Raton, FL, USA, 1985.
14. Margaritondo, G. Characteristics and Properties of Synchrotron Radiation. In *Synchrotron Radiation*; Mobilio, S., Boscherini, F., Meneghini, C., Eds.; Springer: Berlin/Heidelberg, Germany, 2015.
15. Emma, P.; Akre, R.; Arthur, J.; Bionta, R.; Bostedt, C.; Bozek, J.; Brachmann, A.; Bucksbaum, P.; Coffee, R.; Decker, F.-J.; et al. First lasing and operation of an angstrom-wavelength free-electron laser. *Nat. Photonics* **2010**, *4*, 641. [CrossRef]
16. Ratner, D.; Brachmann, A.; Decker, F.J.; Ding, Y.; Dowell, D.; Emma, P.; Fisher, A.; Frisch, J.; Gilevich, S.; Huang, Z.; et al. Second and third harmonic measurements at the linac coherent light source. *Phys. Rev. ST-AB* **2011**, *14*, 060701. [CrossRef]
17. Milton, S.V.; Gluskin, E.; Arnold, N.D.; Benson, C.; Berg, W.; Biedron, S.G.; Borland, M.; Chae, Y.C.; Dejus, R.J.; den Hartog, P.K.; et al. Exponential Gain and Saturation of a Self-Amplified Spontaneous Emission Free-Electron Laser. *Science* **2001**, *292*, 2037. [CrossRef] [PubMed]
18. Biedron, S.G.; Dejusa, R.J.; Huanga, Z.; Milton, S.V.; Sajaeva, V.; Berga, W.; Borlanda, M.; den Hartog, P.K.; Erdmann, M.; Fawleyc, W.M.; et al. Measurements of nonlinear harmonic generation at the Advanced Photon Source's SASE FEL. *Nucl. Instrum. Methods A* **2002**, *483*, 94. [CrossRef]
19. Giannessi, L.; Alesini, D.; Antici, P.; Bacci, A.; Bellaveglia, M.; Boni, R.; Boscolo, M.; Briquez, F.; Castellano, M.; Catani, L.; et al. Self-amplified spontaneous emission for a single pass free-electron laser. *Phys. Rev. ST-AB* **2011**, *14*, 060712. [CrossRef]
20. Henderson, J.R.; Campbell, L.T.; Freund, H.P.; McNeil, B.W.J. Modelling elliptically polarised free electron lasers. *New J. Phys.* **2016**, *18*, 062003. [CrossRef]
21. Freund, H.P.; van der Slot, P.J.M.; Grimminck, D.L.A.G.; Setija, I.D.; Falgari, P. Three-dimensional, time-dependent simulation of free-electron lasers with planar, helical, and elliptical undulators. *New J. Phys.* **2017**, *19*, 023020. [CrossRef]
22. Freund, H.P.; van der Slot, P.J.M. Studies of a terawatt X-ray free-electron laser. *New J. Phys.* **2018**, *20*, 073017. [CrossRef]
23. Zhukovsky, K.; Kalitenko, A. Phenomenological and numerical analysis of power evolution and bunching in single-pass X-ray FELs. *J. Synchrotron Rad.* **2019**, *26*, 159–169. [CrossRef]
24. Zhukovsky, K.J. Two-frequency undulator in a short SASE FEL for angstrom wavelengths. *Optics 20 N* **2018**, *9*, 095003. [CrossRef]
25. Zhukovsky, K. Analysis of harmonic generation in planar and elliptic bi-harmonic undulators and FELs. *Results Phys.* **2019**, *13*, 102248. [CrossRef]
26. Zhukovsky, K.V. Effect of the third undulator field harmonic on spontaneous and stimulated undulator radiation. *J. Synchrotron Rad.* **2019**, *26*, 1481. [CrossRef] [PubMed]
27. Freund, H.P.; van der Slot, P.J.M.J. Variable polarization states in free-electron lasers. *Phys. Commun* **2021**, *5*, 085011. [CrossRef]
28. Zhukovskiy, K.V.; Kalitenko, A.M. Comparative Analysis of Phenomenological and Numerical Modeling of Experiments with Single-Pass Free-Electron Lasers. *Radiophys. Quantum Electron.* **2019**, *62*, 52–64. [CrossRef]
29. Zhukovsky, K.; Kalitenko, A. Harmonic generation in planar undulators in single-pass free electron lasers. *Russ. Phys. J.* **2019**, *62*, 354–362. [CrossRef]
30. Jackson, J.D. Chapter 14. In *Classical Electrodynamics*, 3rd ed; Willey: New York, NY, USA, 1998.
31. Kalitenko, A.M.; Zhukovskii, K.V. Radiation from Elliptical Undulators with Magnetic Field Harmonics. *J. Exp. Theor. Phys.* **2020**, *130*, 327–337. [CrossRef]
32. Zhukovsky, K.V. Undulator and free-electron laser radiation with field harmonics and off-axis effects taken into account analytically. *Phys. Uspekhi* **2021**, *64*, 304. [CrossRef]
33. Zhukovsky, K. Analytical account for the off-axis effects and undulator field harmonics in FELs. *Opt. Laser Technol.* **2020**, *131*. [CrossRef]
34. Zhukovsky, K. X-ray harmonic radiation in free electron lasers with variable deflection parameter of the undulators. *Eur. Phys. J. Plus* **2021**, *136*, 714. [CrossRef]
35. Zhukovsky, K. On the Generation of Even Harmonics in Planar and Elliptical Undulators of Free Electron Lasers. *Ann. Phys.* **2021**, *533*, 2100091. [CrossRef]
36. Zhukovsky, K. Analysis of the spectral properties of free electron lasers in X-RAY and other bands. *Rad. Phys. Chem.* **2021**, *189*, 109698. [CrossRef]
37. Zhukovsky, K. Comparative analysis of the theoretical and experimental spectral properties of X-FELs. *Results Phys.* **2020**, *19*, 103361. [CrossRef]
38. Zhukovsky, K. On the possibilities of amplification and radiation of harmonics in modern X-ray free electron lasers. *Opt. Laser Technol.* **2021**, *143*, 107296. [CrossRef]
39. Zhukovsky, K.; Fedorov, I. Spontaneous and Stimulated Undulator Radiation in Symmetric and Asymmetric Multi-Periodic Magnetic Fields. *Symmetry* **2021**, *13*, 135. [CrossRef]

40. Prakash, B.; Huse, V.; Gehlot, M.; Mishra, G. Analysis of spectral properties of harmonic undulator radiation of an electromagnet undulator. *Optik* **2016**, *127*, 1639. [CrossRef]
41. Zhukovsky, K. Analytical account for a planar undulator performance in a constant magnetic field. *J. Electromagn. Waves Appl.* **2014**, *28*, 1869–1887. [CrossRef]
42. Zhukovsky, K.V. Harmonic Generation by Ultrarelativistic Electrons in a Planar Undulator and the Emission-Line Broadening. *J. Electromagn. Waves Appl.* **2015**, *29*, 132–142. [CrossRef]
43. Dattoli, G.; Mikhailin, V.V.; Zhukovsky, K. Undulator radiation in a periodic magnetic field with a constant component. *J. Appl. Phys.* **2008**, *104*, 124507. [CrossRef]
44. Dattoli, G.; Mikhailin, V.V.; Zhukovsky, K.V. Influence of a constant magnetic field on the radiation of a planar undulator. *Mosc. Univ. Phys. Bull.* **2009**, *64*, 507–512. [CrossRef]
45. Zhukovsky, K.V. Operational solution for some types of second order differential equations and for relevant physical problems. *J. Math. Anal. Appl.* **2017**, *446*, 628–647. [CrossRef]
46. Dattoli, G.; Ottaviani, P.L.; Pagnutti, S. Nonlinear harmonic generation in high-gain free-electron lasers. *J. Appl. Phys.* **2005**, *97*, 113102. [CrossRef]
47. Dattoli, G.; Giannessi, L.; Ottaviani, P.L.; Ronsivalle, C. Semi-analytical model of self-amplified spontaneous-emission free-electron lasers, including diffraction and pulse-propagation effects. *J. Appl. Phys.* **2004**, *95*, 3206–3210. [CrossRef]
48. Giannessi, L. Seeding and Harmonic Generation in Free-Electron Lasers. In *Synchrotron Light Sources and Free-Electron Lasers*; Jaeschke, E.J., Ed.; Springer International Publishing: Cham, Switzerland, 2016. [CrossRef]
49. Xie, M. Exact and variational solutions of 3D eigenmodes in high gain FELs. *Nucl. Instrum. Methods A* **2000**, *445*, 59. [CrossRef]
50. Xie, M. Design optimization for an X-ray free electron laser driven by SLAC linac. In Proceedings of the 1995 Particle Accelerator Conference IEEE, Piscataway, NJ, USA, 1–5 May 1995; pp. 183–185.
51. Bonifacio, R.; de Salvo, L.; Pierini, P. Large harmonic bunching in a high-gain free-electron laser. *Nucl. Instrum. A* **1990**, *293*, 627. [CrossRef]
52. Huang, Z.; Kim, K.-J. Nonlinear harmonic generation of coherent amplification and self-amplified spontaneous emission. *Nucl. Instrum. Methods A* **2001**, *475*, 112. [CrossRef]
53. Geloni, G.; Saldin, E.; Schneidmiller, E.; Yurkov, M. Exact solution for second harmonic generation in XFELs. *Opt. Comm.* **2007**, *271*, 207. [CrossRef]
54. Tanaka, T.; Kitamura, H. SPECTRA: A synchrotron radiation calculation code. *J. Synchrotron Rad.* **2001**, *8*, 1221–1228. [CrossRef]
55. Tanaka, T. Numerical methods for characterization of synchrotron radiation based on the Wigner function method. *Phys. Rev. ST Accel. Beams* **2014**, *17*, 060702. [CrossRef]
56. Tanaka, T. Coherent mode decomposition using mixed Wigner functions of Hermite–Gaussian beams. *Opt. Lett.* **2017**, *42*, 1576. [CrossRef]
57. Tanaka, T. Universal representation of undulator phase errors. *Phys. Rev. AB* **2018**, *21*, 110704. [CrossRef]